



Published in final edited form as:

Nat Chem. 2015 May ; 7(5): 431–437. doi:10.1038/nchem.2237.

Structure and biosynthesis of a macrocyclic peptide containing an unprecedented lysine-to-tryptophan crosslink

Kelsey R. Schramma^{#1}, Leah B. Bushin^{#1}, and Mohammad R. Seyedsayamdost^{1,2,*}

¹Department of Chemistry, Princeton University, Princeton, New Jersey, USA

²Department of Molecular Biology, Princeton University, Princeton, New Jersey, USA

These authors contributed equally to this work.

Abstract

Streptococcal bacteria use peptide signals as a means of intraspecies communication. These peptides can contain unusual post-translational modifications providing opportunities for expanding our understanding of Nature's chemical and biosynthetic repertoires. Herein we have combined tools from natural products discovery and mechanistic enzymology to report the structure and biosynthesis of streptide, a streptococcal macrocyclic peptide. We show that streptide bears an unprecedented post-translational modification involving a covalent linkage between two unactivated carbons within the side chains of lysine and tryptophan. The biosynthesis of streptide was addressed by genetic and biochemical studies. The former implicated a new SPASM domain-containing radical SAM enzyme, StrB, while the latter revealed that StrB contains two [4Fe-4S] clusters and installs the unusual lysine-to-tryptophan crosslink in a single step. By intramolecularly stitching together the side chains of lysine and tryptophan, StrB provides a new route for biosynthesizing macrocyclic peptides.

Nature has evolved a multitude of biosynthetic strategies for generating cyclic peptides¹. The ordinary *N*-to-*C*-terminal cyclization via amide bond formation has been well-documented², as have the biosyntheses of peptides cyclized by isopeptide bonds³, disulfide bonds⁴, esters^{5,6}, and thiolactones^{7,8}. More exotic strategies, such as heterolytic or homolytic mechanisms for formation of thioether-cyclized peptides, exemplified by nisin⁹ and subtilisin¹⁰, have also been demonstrated, as have production of carbacyclic peptides in the labyrinthopeptins¹¹ and P450-mediated bis-aryl cross-coupling reactions in the glycopeptides¹², such as vancomycin. These and other exemplars have provided fascinating cases of unusual peptide structures and their corresponding biosynthetic pathways^{1,13}. Herein we report the structure and biosynthesis of a macrocyclic peptide that does not fall

Reprints and permission information is available online at <http://npg.nature.com/reprintsandpermission/>.

*Correspondence and requests for materials should be addressed to M.R.S. mrseyed@princeton.edu.

Author Contributions

K.R.S., L.B.B. and M.R.S. designed and executed experiments, and analyzed data. M.R.S. conceived of the project and wrote the manuscript.

Additional Information

The authors declare no competing financial interest. Supplementary information accompanies this paper at www.nature.com/naturechemistry.

into any of the categories above and thus represents the founding member of a new family of naturally-occurring cyclic peptides. It is produced by the pathogenic model *Streptococcus thermophilus* and bears a lysine-to-tryptophan crosslink, which is installed in a single step at unactivated side chain carbons by a metalloenzyme.

S. thermophilus is a non-pathogenic streptococcal model strain used in the fermentation of dairy products. While it does not express the virulence factors of its pathogenic relatives, which include *Streptococcus mitis*, *Streptococcus pyogenes*, and *Streptococcus pneumoniae*, it does harbor a new, recently-identified quorum sensing system common to many streptococci, including pathogenic strains. Pioneering studies by Monnet and coworkers have elucidated the features of this system (Fig. 1a)¹⁴⁻¹⁶. A short hydrophobic peptide (SHP, H₂N-EGIIVVVGCOOH) is produced as a pheromone and released into the environment. At threshold concentrations, SHP is imported into the cytoplasm by the Ami oligopeptide transporter, where it modulates gene expression upon binding to a stand-alone transcriptional regulator, Rgg, which itself is divergently transcribed from *shp* (Fig. 1a)¹⁴⁻¹⁶. Rgg proteins have been shown to regulate, among other processes, competence, the production of proteinase virulence factors and bacteriocins, as well as stress response¹⁷⁻²¹. One of the loci upregulated by the *shp/rgg* quorum sensing system in *S. thermophilus* is the subject of this report^{14,15}. We propose the name *str* for this gene cluster. It consists of gene STER_1357, STER_1356, and STER_1355, which, respectively, code for a short precursor peptide (*strA*), a radical S-adenosylmethionine (SAM) enzyme (*strB*), and a putative transporter (*strC*) (Fig. 1a)^{14,15}. Previous studies by the Monnet group demonstrated that the 30mer precursor peptide, the product of *strA*, was modified to a mature 9mer (H₂N-AK²GDGW⁶KVM-COOH), termed Pep1357C. While it was shown that residues K² and W⁶ were involved in the cyclization¹⁴, the detailed structure of the mature peptide, for which we propose the name streptide, has remained unknown as has the role, if any, of the radical SAM enzyme in its biosynthesis.

Results and Discussion

Structural Elucidation of Streptide

We began our studies by attempting to structurally elucidate the product of the *str* cluster. *S. thermophilus* is a facultative aerobe and large-scale streptide production cultures needed to be prepared under micro-aerophilic conditions. Mass- and UV-guided fractionation, using the reported m/z of 989,¹⁴ allowed isolation of streptide in quantities sufficient for NMR analysis. A suite of one- and two-dimensional NMR spectra were analyzed to solve the structure of streptide (Fig. 1b, Supplementary Fig. 1-7, Supplementary Table 1). ¹H, COSY, and TOCSY spectra revealed the presence of seven unmodified residues: an N-terminal Ala, two Gly residues, Asp, Lys, Val, and a C-terminal Met, consistent with the sequence previously reported.¹⁴ The remaining K² and W⁶ residues were modified. NMR spectral analyses indicated that K² and W⁶ lacked a β-¹H and the aromatic C7-¹H, respectively. HMBC data showed clear correlations from the remaining β-¹H of K² to the aromatic C6, C7, and C8 carbons of W⁶. Likewise, the C6-¹H of the Trp side chain showed correlations to Cβ of K² establishing the presence of a Lys-to-Trp crosslink through a C-C bond between the Cβ of K² and the aromatic C7 of W⁶ (Fig. 1b, c). NOESY spectra exhibited several cross

peaks between the α -, β -, and γ - ^1H s of K^2 to the indole ring protons of W^6 and were consistent with this unique modification. In addition, comparison of the ^1H and ^{13}C chemical shift patterns in streptide with those of 4-methyl-indole, 7-methyl-indole, and 7-methyl-tryptophan verified this assignment and established that the modification occurs at the C7 position of the Trp side chain, and not at the C4 (Supplementary Fig. 8).

To further corroborate the structure of streptide, high-resolution (HR) HPLC-ESI-MS and tandem HR-MS experiments were carried out. HR-MS data yielded $[\text{M}+\text{H}]^+_{\text{obs}}$ of 989.4870 consistent with the structure in Fig. 1c ($[\text{M}+\text{H}]^+_{\text{calc}}$ 989.4879). Collision-induced dissociation provided further evidence for the structure of streptide, notably the b6, b7, b8, y1, and y3 ions (Supplementary Fig. 9). No fragments were observed within the first six *N*-terminal residues supporting the cyclic structure of streptide via side chain connectivity between the second and sixth residues. Collectively, the NMR and HR-MS data convincingly support a post-translational modification that involves cyclization by an unprecedented Lys-to-Trp covalent bond.

A Computational Model of Streptide

The unusual macrocycle generated by the Lys-to-Trp crosslink in streptide marks a new structural motif for cyclic peptides. The three-dimensional conformation of streptide was modeled to address the unique structural constraints imposed by the macro-cyclization as well as the stereochemistry of the newly-formed chiral center at the $\text{C}\beta$ of K^2 . Vederas and colleagues have successfully used this approach to distinguish between possible diastereomers in the post-translationally-modified peptides subtilosin and the thuricin family of bacteriocins²²⁻²⁵. To do so, Marfey's analysis was first carried out and indicated that all residues contained the L stereoconfiguration at their α -carbons (see Supplementary Information). Next, NMR NOESY correlations were used in conjunction with the CYANA algorithm, which utilizes molecular dynamics simulations in torsion angle space, to minimize a target function (*f*) that measures agreement between computed structures and constraints derived from NOESY²²⁻²⁷. A low target function indicates a good match between the calculated structure and the given set of constraints. Several parameters were tested to optimize the number of constraints for structure calculations. A NOESY spectrum acquired in $\text{H}_2\text{O}/\text{D}_2\text{O}$ at 298 K with a mixing time of 500 ms optimized the number of cross-peaks while avoiding spin diffusion and was therefore utilized for CYANA calculations (Supplementary Fig. 4). The Lys-to-Trp covalent modification was incorporated into CYANA separately and contained either the R or S configuration at the $\text{C}\beta$ of K^2 (see Supplementary Information). The S configuration exhibited a significantly better fit to the data with favorable *f* ($0.042 \pm .0003$ for S, $0.054 \pm .0005$ for R) and rmsd values (1.62 \AA for S, 1.72 \AA for R), while also accounting for a greater number of NOESY-derived distance constraints, relative to the R epimer (29 for S, 27 for R, Supplementary Table 2). The top 5 calculated structures as determined by the target function (Supplementary Fig. 10), along with the best structure (Fig. 1d), indicate a rigid cyclic structure held in place by the bridging, modified indole side chain as well as possible H-bonds emanating from the Asp side chain (D^4) within the macrocycle. This rigid macrocycle is likely important for interactions with downstream protein receptors. The C-terminal tail, on the other hand, shows significant flexibility. Together, the studies above provide a conformational model for

streptide and indicate that the crosslink is generated with the S configuration at the C β of K² (Fig. 1c), a prediction that can be tested experimentally in the future.

Proposed Role for StrB

Having fully elucidated the structure of streptide, we considered its biogenesis and suspected that StrB, the lone modification enzyme in the streptide gene cluster, was responsible for formation of the Lys-to-Trp crosslink. To assess this hypothesis, we first took a genetic approach. StrB was inactivated by insertional mutagenesis of an erythromycin resistance gene (*ery*) into the *S. thermophilus* chromosome (Supplementary Table 3)¹⁵. Differential HPLC-MS profiles of the resulting mutant strain, *strB::ery*, compared with wt *S. thermophilus*, clearly showed that streptide production is abolished in the mutant indicating that StrB is essential for its biosynthesis (Fig. 1e). The precursor peptide StrA was not observed in these experiments suggesting it was degraded in the absence of StrB or not secreted as a premature product. In light of these results and the logic within the radical SAM-modified ribosomal peptides, which have been bioinformatically analyzed in detail^{28,29}, we propose that the 30mer peptide is acted upon by StrB to install the Lys-to-Trp crosslink. The resulting product is then further processed by one or two proteases, likely involving StrC, to give the final cyclic streptide (Fig. 2).

StrB is a Functional Radical SAM Enzyme

Biochemical studies were initiated to further define the role of StrB in the biogenesis of streptide. StrB belongs to the radical SAM enzyme superfamily, members of which catalyze a number of important and difficult transformations in primary and secondary metabolism³⁰⁻³². They employ a [4Fe-4S]⁺ cluster, held in place by a canonical CxxxCxxC motif, to reductively activate SAM and generate L-Met and a 5'-deoxyadenosyl 5'-radical (5'-dA•). The latter initiates catalysis by abstraction of a hydrogen atom from its substrate³⁰⁻³². Recently, a subfamily of radical SAM enzymes, which contain C-terminally extended domains, has been identified by Haft and Basu^{28,29}. These enzymes make up the so-called SPASM domain subfamily³³ and appear to be involved in the modification of ribosomally-generated peptides. The SPASM domain consists of a conserved C-terminal motif that allows binding of at least one additional [4Fe-4S] cluster (Fig. 3a)^{28,29}. The anaerobic sulfatase, anSME, is the best-characterized SPASM-domain enzyme³⁴⁻³⁸. It was recently shown that eight Cys residues within the SPASM motif bind two auxiliary FeS clusters, named AuxI and AuxII³⁸⁻³⁹. Sequence alignments of the SPASM motif in StrB with that of anSME disclose that StrB lacks a critical Cys residue in the AuxI site. We therefore hypothesized that StrB would harbor one auxiliary cluster, bound by its modified SPASM motif (Fig. 3a), as well as the canonical radical SAM-activating cluster, common to all radical SAM enzymes.

StrB was cloned and expressed as a hexa-His-StrB construct in an *E. coli* host^{40,41}. An optimized procedure provided 10 mg of StrB per g of *E. coli* cell paste. As-isolated StrB contained 7.0 ± 0.1 Fe and 4.6 ± 0.7 S per polypeptide. Subsequent reconstitution provided 8.5 ± 0.4 Fe and 7.1 ± 0.5 S per polypeptide suggesting that StrB contains two [4Fe-4S] clusters, in line with the proposal above. UV-vis and X-band EPR spectra after reduction with sodium dithionite (DT, Na₂S₂O₄) are shown in Fig 3. The observed 320 nm shoulder

and broad visible band at 395 nm are consistent with the presence of [4Fe-4S] clusters (Fig. 3b). Further, the EPR spectrum of the DT-reduced StrB in the absence of SAM exhibits a signal with rhombic symmetry, with g values of 2.05, 1.94, and 1.87 (Fig. 3c). While similar to the signal reported for PqqE⁴², this spectrum varies from the usual axial signal observed for most radical SAM enzymes³⁰⁻³². To examine if this spectrum consisted of composite signals of two FeS clusters, we created a double Cys-to-Ala mutant in the site proposed to bind AuxII, the second auxiliary cluster (Fig. 3a). This mutant, C409A/C415A-StrB, contained 3.5 ± 0.1 Fe and 3.8 ± 0.2 S per polypeptide. In vitro reconstitution did not significantly increase the contents of Fe (4.5 ± 0.1) and labile S (4.3 ± 0.1). The EPR signal exhibits axial symmetry with g values of 2.06 and 1.93 (Fig. 3d), very similar to the SAM-cleaving FeS clusters from other radical SAM enzymes. On the basis of EPR spectral analyses and Fe/S quantitation with the C409A/C415A-mutant and wt proteins, we propose that StrB – like subfamily-members BtrN,⁴³ AlbA,¹⁰ and SkfB⁴⁴ – contains two 4Fe-4S clusters, one that can reductively activate SAM (see below), and a second auxiliary cluster held in place by the StrB SPASM motif. The spectrum in Fig. 3c is a composite signal of these two clusters. That the auxiliary cluster is redox-active may be important for the mechanism of StrB (see below). EPR quantitation yields 0.3 spins per polypeptide, suggesting that reduction is incomplete, a common phenomenon for radical SAM enzymes.

A hallmark of radical SAM enzymes is their ability to produce L-Met and 5'-deoxyadenosine (5'-dA) even in the absence of substrate. Reaction of DT-reduced StrB with SAM indeed yielded catalytic and time-dependent formation of 5'-dA, as verified by comparison with authentic 5'-dA using HR-HPLC-ESI-MS analysis (Supplementary Fig. 11). Thus, StrB is a functional radical SAM enzyme, which contains an N-terminal SAM-activating [4Fe-4S] cluster and an additional C-terminal auxiliary cluster.

Lys-to-Trp Crosslinking Catalyzed by StrB

To assess the reaction catalyzed by StrB, we synthesized the 30mer StrA, as well as truncated 20mer and 9mer substrates, using solid-phase peptide synthesis (Fig. 2). Subsequent activity assays were initiated by SAM and monitored by HR-HPLC-ESI-MS and tandem HR-MS utilizing DT as reductant. No products were observed with the truncated 20mer and 9mer peptides, indicating that the leader sequence is essential for catalysis by StrB and that Lys-to-Trp crosslink formation precedes proteolysis to generate the mature 9mer. Assays with full-length StrA revealed a SAM-, StrB-, reductant-, and time-dependent formation of a new peptide species lacking two protons ($[M+3H]^{+3}_{\text{calc}}$ 1104.53023, $[M+3H]^{+3}_{\text{obs}}$ 1104.53157, Fig. 4a, Supplementary Table 4). This was accompanied by nearly stoichiometric loss of StrA and formation of 5'-dA relative to the peptide product, indicating that SAM is reductively activated during the course of the reaction and used as a co-substrate rather than a cofactor (Supplementary Fig. 12). No products were observed with the C409A/C415A-StrB mutant, which does not harbor the auxiliary cluster, indicating its requirement for catalysis (Supplementary Fig. 13). These data demonstrate that StrB acts on StrA in a leader-peptide dependent fashion^{1,45}, and that StrB consumes one mole of SAM per mole of product-30mer and 5'-dA formed. Preliminary steady-state kinetic studies show parameters for $V_{\text{max}}/[E_T]$ and K_m of 0.14 min^{-1} and $160 \mu\text{M}$, respectively.

To ensure that StrB installed the same modification as that observed in the mature 9mer (Fig. 1c), the reaction was carried out on a large scale, the product 30mer isolated and assessed by ^1H , gCOSY, and TOCSY NMR spectra, and by tandem HR-MS. The TOCSY spectral comparison of substrate-30mer and product-30mer reveals a Trp side chain modified at the indole-C7 position only in the product-30mer, a modification that is similar to that observed in the 9mer (Fig. 4b). The 30mer substrate, on the other hand, only exhibits signals for two unmodified Trp residues. Further analysis of the product 30mer shows a Lys residue modified at the β -carbon, again consistent with the structure of streptide (Supplementary Fig. 14). Additional compelling evidence was provided by tandem HR-MS, which exhibited fragmentation to all possible b and y ions, except for those in the 5-residue macrocycle generated by the Lys-to-Trp crosslink comprising the KGDGW sequence (Fig. 4c, Supplementary Table 5). Our results thus verify that StrB, in a single step, modifies the 30mer StrA to install a C-C bond between the side chains of Lys and Trp.

StrB Mechanism

Having established the reaction catalyzed by StrB, we investigated its mechanism further by positing that the lysyl β -methylene hydrogen is removed during the course of catalysis. To test this mechanism, the 30mer precursor peptide was synthesized with a $^2\text{H}_8$ -L-Lys, in which the side-chain was uniformly deuterated (Fig. 2, K). Analysis of the reaction products of this $^2\text{H}_8$ -K-30mer with StrB revealed deuterated 5'-dA ($5'\text{-}^2\text{H}\text{-}5'\text{-dA}$) as product ($[\text{M} + \text{H}]^+_{\text{calc}} 253.11539$, $[\text{M} + \text{H}]^+_{\text{obs}} 253.11509$, Supplementary Table 4) as well as a 30mer product containing 7 deuterons ($[\text{M} + 3\text{H}]^{+3}_{\text{calc}} 1106.87766$, $[\text{M} + 3\text{H}]^{+3}_{\text{obs}} 1106.87840$), both entirely in agreement with abstraction of the β -methylene hydrogen by the 5'-dA•.

Comparisons with protonated StrA after 2-3 turnovers did not reveal a kinetic isotope effect ($^{\text{H}}\text{V}/^{\text{D}}\text{V} \sim 1$, Supplementary Fig. 15). The low turnover number coupled with a lack of an isotope effect may collectively suggest that multiple turnover is limited by re-reduction with the non-natural redox reagent DT in our assays, or conformational changes related to this step in the catalytic cycle.

The results above allow us to propose a mechanistic model for StrB (Fig. 5). In this model, reductive activation of SAM leads to formation of 5'-dA•, which abstracts a β -hydrogen of Lys, thus generating a lysyl radical⁴⁶. This intermediate reacts with the indole side chain to generate an indolyl radical bearing the Lys-to-Trp crosslink. Loss of proton and rearomatization concomitant with reduction of the auxiliary Fe-S cluster gives rise to crosslinked StrA. Our model assigns a redox role to the auxiliary Fe-S cluster, which is active in the +2 oxidation state but is converted to the +1 form during the course of catalysis. The active site cluster, which reductively cleaves SAM, is active in the +1 oxidation state but is converted to the +2 form after generation of the 5'-dA•. After one turnover, intramolecular electron transfer from the auxiliary Fe-S cluster to the other would render both in the active oxidation state. Alternatively, each could undergo separate redox reactions with a diffusible redox partner. The issue of regenerating redox states of multiple FeS clusters in radical SAM enzymes has been addressed in DesII⁴⁷, and most recently by elegant structural and biochemical studies with anSME³⁹ and BtrN^{43,48}. Similar studies will be necessary to clarify this facet of StrB catalysis.

Prevalence of the *str* cluster

With the insights at hand regarding the structure and biosynthesis of streptide, we addressed its prevalence in bacterial genomes, especially as streptide production is regulated by the *shp-rgg* quorum sensing system, which has been shown to be wide-spread in lactic acid bacteria^{15,16}. Thorough bioinformatic studies by Haft have led to the annotation of StrA as a member of the KxxxW peptides, contained in the TIGRFAM model TIGR04079²⁸. These genes code for KxxxW-containing peptides and co-occur with a maturase radical SAM enzyme (TIGR04080), represented by StrB in the *str* cluster. To better understand the prevalence of the *str* gene cluster, we examined the available finished bacterial genome databases for the presence of *strA* and *strB*. These searches excluded metagenomic and draft genome sequences to avoid discrepancies as a result of poor or incomplete sequence data. Searches with *strA* as query showed that several *S. thermophilus* strains, *Lactococcus lactis*, as well as the human pathogen *S. mitis*, the causative agent of endocarditis⁴⁹, harbor both genes. The precursor peptide is aptly annotated as belonging to the KxxxW family in these cases²⁸. Searches with *strB* as a query sequence, led to identification of additional strains that contain *str*, notably several *S. agalactiae* species, human pathogens belonging to the Group B streptococcus category, as well as *Streptococcus suis*, a zoonotic infectious agent (Supplementary Fig. 16)^{50,51}. These *strB* sequences were not accompanied by *strA*. Inspection for an ORF upstream of *strB* revealed that all *S. agalactiae* and *S. suis* sequences do in fact code for *strA* as well as the *shp* quorum sensing system, but that these small genes were missed in the automated gene prediction process (Supplementary Fig. 16). Comparisons among a total of 28 *strA* sequences uncovered in this fashion, which include 18 previously missed *strA* ORFs in the pathogens *S. agalactiae* and *S. suis*, reveal a high degree of similarity and the conserved signature motif of VLE-(S/N)-SS-(M/I)-AKGDGW-(K/A) in StrA (Supplementary Fig. 16). The underlined –KGDGW– sequence comprising the crosslinked K and W residues in the macrocycle is entirely conserved in this subset of molecules. Thus, the *str* cluster is wide-spread and, aside from *S. thermophilus* and *L. lactis*, at least three human pathogens, *S. mitis*, *S. agalactiae* and *S. suis*, have the potential to produce streptide. All strains also contain the *shp-rgg* quorum sensing system directly upstream of *str*, suggesting that streptide production occurs in a cell density-dependent fashion in these pathogens.

Conclusions

Radical SAM enzymes have been shown to catalyze an impressive array of reactions and despite their relatively recent discovery, they have advanced to one of the most versatile enzyme families in Nature. Herein we report a new example of this versatility by demonstrating a unique side chain crosslinking reaction in streptide and proposing a radical mechanism for its formation. By stitching together unactivated carbons in the Lys and Trp amino acid side chains, StrB contributes to the production of a family of cyclic peptides that are both novel and wide-spread in a number of human pathogens. Aside from the important biological implications, the studies above demonstrate that targeted analysis of biosynthetic gene clusters, which harbor radical SAM enzymes, presents enticing opportunities for finding novel chemistries, both within small molecules and their exotic biosynthetic reaction mechanisms.

Methods

Materials and procedures for structural elucidation of streptide, Marfey's analysis, structure calculations, insertional mutagenesis to generate *strB::ery*, cloning and expression of StrB, determination of the concentration of StrB and the contents of its labile Fe and S, EPR spectroscopy, synthesis and purification of StrA, synthesis of Fmoc-3,3,4,4,5,5,6,6-²H₈-Lys(Boc)-OH, and the corresponding ²H₈-K-StrA are provided in the Supplementary Information.

Bacterial production and purification of streptide

Streptococcus thermophilus LMD-9 was obtained from ATCC. Colonies from an agar plate on Brain Heart Infusion agar were used to inoculate a small overnight culture in a sterile 14 mL culture tube containing 13 mL of Brain Heart Infusion medium. The culture was grown statically at 42°C overnight. 250 mL bottles, each containing 225 mL of chemically defined medium (see Supplementary Information), were inoculated with 3 mL of overnight culture and grown statically at 42°C for 12-16 hours. After reaching an OD_{600 nm} = 0.7-1.0, large-scale cultures of *S. thermophilus* (8 L total) were centrifuged at 12,000 × g for 25 min and the remaining supernatant further clarified using 0.2 micron Corning filter units. The filtered supernatant was passed through a C18-functionalized silica gel column (8 g, 10 mL bed volume), which had been washed with MeCN and equilibrated with H₂O supplemented with 0.1% TFA (H₂O-TFA). Following application of the filtered supernatant, the column was washed with H₂O-TFA and bound material eluted with 60% MeCN in H₂O-TFA and finally with 100% MeCN. The 60% fraction was dried in vacuo, resuspended in H₂O-TFA, and purified on a preparative Agilent Eclipse XCB-C8 column (7 μm, 250 × 21.2 mm) operating at 13 mL/min. Elution was carried out with an isocratic step (10 min, 5% MeCN in H₂O) followed by a gradient from 5–30% MeCN over 10 minutes, and finally a gradient from 30–100% MeCN over 10 minutes. Both MeCN and H₂O contained 0.1 % formic acid. Streptide eluted at 10–12.5 % MeCN. Fractions containing streptide, as judged by HPLC-MS, were pooled, dried, and resuspended in H₂O-TFA and further purified on a semi-preparative Phenomenex Luna C18 column (5 μm, 10 × 250 mm) operating at 2.5 mL/min. Streptide was eluted isocratically (10 min, 7% MeCN in H₂O+0.1% formic acid) followed by application of a gradient from 7–30% MeCN over 15 minutes. Streptide eluted at 12–14% MeCN. Fractions containing streptide were pooled, dried, and resuspended in H₂O-TFA. Reapplication of this material onto the same semi-preparative column using the same flow rate and elution program afforded 0.3 mg of pure material suitable for NMR analysis.

Synthesis of 30mer substrate (StrA) by SPPS

Syntheses of the substrate 30mer, StrA, and of truncated substrates (9mer and 20mer) were carried out using solid phase peptide synthesis with HATU as coupling reagent. Standard Fmoc- and side-chain-protected amino acids were used. Asp-Gly and Glu-Ser sequences were incorporated as a Fmoc-Asp(OtBu)-(Dmb)Gly-OH and Fmoc-Glu(OtBu)-Ser(ψ^{Me,Me}Pro)-OH dipeptides, respectively. The Kaiser test was used to determine completion of each coupling reaction.

Activity assays of StrB

StrB activity assays were performed in an inert atmosphere. Reactions were typically carried in a 0.5 mL Eppendorf tube on a 150 μ L scale and contained assay buffer (50 mM HEPES, 100 mM KCl, 10% glycerol, pH 7.5), 25 or 10 μ M StrB, 2 mM $\text{Na}_2\text{S}_2\text{O}_4$, 0.75 mM SAM, and varying concentrations of StrA (0-500 μ M). The reaction was initiated by the addition of SAM. At each time point, 25 μ L were removed, and quenched by mixing with 25 μ L of 100 mM H_2SO_4 . The quenched samples were taken out of the glove box, precipitated StrB removed by centrifugation, and the supernatant resolved on a Strata-C8 SPE column (Phenomenex, 30 mg), which had been washed with MeCN and equilibrated in $\text{H}_2\text{O}+0.1\%$ formic acid. After loading, the column was washed with 2 mL H_2O and the peptide eluted with 1.5 mL 50% MeCN and 0.5 mL of 100% MeCN. The eluates were combined, evaporated to dryness in a speedvac, re-dissolved in 200 μ L of 10% MeCN (+0.1% formic acid) and analyzed by Qtof-HPLC-MS (see Supplementary Information). Substrate and product typically eluted at 42% and 39% MeCN, respectively. The flowthrough from the Strata-C8 SPE column, which contained 5'-dA, was also dried in a speedvac, then re-dissolved in 100 μ L H_2O (+0.1% formic acid) and analyzed by HPLC on an analytical Phenomenex Luna C18 column (5 μ m, 4.6 \times 100 mm) using isocratic elution at 6% MeCN in H_2O . Substrate StrA, product, and 5'-dA, were quantified by generating standard curves with known concentrations of each component, which were determined spectrophotometrically.

Supplementary Material

Refer to Web version on PubMed Central for supplementary material.

Acknowledgments

We thank Istvan Pelczer and Ken Connover at the Princeton Chemistry NMR facility for assistance with NMR data acquisition, Squire Booker for the kind gift of pDB1282, and Zachary Brown for advice regarding peptide synthesis. This work was supported by the National Institutes of Health Grant GM098299 (to M.R.S.) and by Princeton University start-up funds.

References

1. Arnison PG, et al. Ribosomally synthesized and post-translationally modified peptide natural products: overview and recommendations for a universal nomenclature. *Nat. Prod. Rep.* 2013; 30:108–160. [PubMed: 23165928]
2. Trauger JW, Kohli RM, Mootz HD, Marahiel MA, Walsh CT. Peptide cyclization catalysed by the thioesterase domain of tyrocidine synthetase. *Nature.* 2000; 407:215–218. [PubMed: 11001063]
3. Duquesne S, et al. Two enzymes catalyze the maturation of a lasso peptide in *Escherichia coli*. *Chem. Biol.* 2007; 14:793–803. [PubMed: 17656316]
4. Dorenbos R, et al. Thiol-disulfide oxidoreductases are essential for the production of the lantibiotic sublancin 168. *J. Biol. Chem.* 2002; 277:16682–16688. [PubMed: 11872755]
5. Ziemert N, Ishida K, Liaimer A, Hertweck C, Dittmann E. Ribosomal synthesis of tricyclic depsipeptides in bloom-forming cyanobacteria. *Angew. Chem. Int. Ed.* 2008; 47:7756–7759.
6. Philmus B, Christiansen G, Yoshida WY, Hemscheidt TK. Post-translational modification in microviridin biosynthesis. *ChemBioChem.* 2008; 9:3066–3073. [PubMed: 19035375]
7. Ji G, Beavis RC, Novick RP. Bacterial interference caused by autoinducing peptide variants. *Science.* 1997; 276:2027–2030. [PubMed: 9197262]

8. Mayville P, et al. Structure-activity analysis of synthetic autoinducing thiolactone peptides from *Staphylococcus aureus* responsible for virulence. *Proc. Natl. Acad. Sci. USA.* 1999; 96:1218–1223. [PubMed: 9990004]
9. Li B, et al. Structure and mechanism of the lantibiotic cyclase involved in nisin biosynthesis. *Science.* 2006; 311:1464–1467. [PubMed: 16527981]
10. Flühe L, et al. The radical SAM enzyme AlbA catalyzes thioether bond formation in subtilisin A. *Nat. Chem. Biol.* 2012; 8:350–357. [PubMed: 22366720]
11. Müller WM, Schmiederer T, Enslé P, Süßmuth RD. In vitro biosynthesis of the prepeptide of type-III lantibiotic labyrinthopeptin A2 Including formation of a C-C bond as a post-translational modification. *Angew. Chem. Int. Ed.* 2010; 49:2436–2440.
12. Zerbe K, et al. An oxidative phenol coupling reaction catalyzed by OxyB, a Cytochrome P450 from the vancomycin-producing microorganism. *Angew. Chem. Int. Ed.* 2004; 43:6709–6713.
13. Dunbar KL, Mitchell DA. Revealing nature's synthetic potential through the study of ribosomal natural product biosynthesis. *ACS Chem. Biol.* 2013; 8:473–487. [PubMed: 23286465]
14. Ibrahim M, et al. Control of the transcription of a short gene encoding a cyclic peptide in *Streptococcus thermophilus*: a new quorum-sensing system? *J. Bacteriol.* 2007; 189:8844–8854. [PubMed: 17921293]
15. Fleuchot B, et al. Rgg proteins associated with internalized small hydrophobic peptides: a new quorum-sensing mechanism in streptococci. *Mol. Microbiol.* 2011; 80:1102–1119. [PubMed: 21435032]
16. Gardan R, Besset C, Guillot A, Gitton C, Monnet V. The oligopeptide transport system is essential for the development of natural competence in *Streptococcus thermophilus* strain LMD-9. *J. Bacteriol.* 2009; 191:4647–4655. [PubMed: 19447907]
17. Lyon WR, Gibson CM, Caparon MG. A role for trigger factor and an rgg-like regulator in the transcription, secretion and processing of the cysteine proteinase of *Streptococcus pyogenes*. *EMBO J.* 1998; 17:6263–6275. [PubMed: 9799235]
18. Chaussee MS, Ajdic D, Ferretti JJ. The rgg gene of *Streptococcus pyogenes* NZ131 positively influences extracellular SPE B production. *Infect. Immun.* 1999; 67:1715–1722. [PubMed: 10085009]
19. Mashburn-Warren L, Morrison DA, Federle MJ. A novel double-tryptophan peptide pheromone controls competence in *Streptococcus* spp. via an Rgg regulator. *Mol. Microbiol.* 2010; 78:589–606. [PubMed: 20969646]
20. Fernandez A, Borges F, Gintz B, Decaris B, Leblond-Bourget N. The rggC locus, with a frameshift mutation, is involved in oxidative stress response by *Streptococcus thermophilus*. *Arch. Microbiol.* 2006; 186:161–169. [PubMed: 16847652]
21. Qi F, Chen P, Caufield PW. Functional analyses of the promoters in the lantibiotic mutacin II biosynthetic locus in *Streptococcus mutans*. *Appl. Environ. Microbiol.* 1999; 65:652–658. [PubMed: 9925596]
22. Kawulka KE, et al. Structure of subtilisin A, a cyclic antimicrobial peptide from *Bacillus subtilis* with unusual sulfur to alpha-carbon cross-links: formation and reduction of alpha-thio-alpha-amino acid derivatives. *Biochemistry.* 2004; 43:3385–3395. [PubMed: 15035610]
23. Rea MC, et al. Thuricin CD, a posttranslationally modified bacteriocin with a narrow spectrum of activity against *Clostridium difficile*. *Proc. Natl. Acad. Sci. USA.* 2010; 107:9352–9357. [PubMed: 20435915]
24. Sit CS, McKay RT, Hill C, Ross RP, Vederas JC. The 3D structure of thuricin CD, a two-component bacteriocin with cysteine sulfur to α -carbon cross-links. *J. Am. Chem. Soc.* 2011; 133:7680–7683. [PubMed: 21526839]
25. Sit CS, van Belkum MJ, McKay RT, Worobo RW, Vederas JC. The 3D solution structure of thuricin H, a bacteriocin with four sulfur to α -carbon crosslinks. *Angew. Chem. Int. Ed.* 2011; 50:8718–8721.
26. Güntert P, Mumenthaler C, Wüthrich K. Torsion angle dynamics for NMR structure calculation with the new program DYANA. *J. Mol. Biol.* 1997; 273:283–298. [PubMed: 9367762]

27. Herrmann T, Güntert P, Wüthrich K. Protein NMR structure determination with automated NOE-identification in the NOESY spectra using the new software ATNOS. *J. Biomol. NMR.* 2002; 24:171–189. [PubMed: 12522306]
28. Haft DH, Basu MK. Biological systems discovery in silico: radical S-adenosylmethionine protein families and their target peptides for posttranslational modification. *J. Bacteriol.* 2011; 193:2745–2755. [PubMed: 21478363]
29. Haft DH. Bioinformatic evidence for a widely distributed, ribosomally produced electron carrier precursor, its maturation proteins, and its nicotinoprotein redox partners. *BMC Genomics.* 12:21–34. [PubMed: 21223593]
30. Frey PA, Booker SJ. Radical mechanisms of S-adenosylmethionine-dependent enzymes. *Adv. Protein Chem.* 2001; 58:1–45. [PubMed: 11665486]
31. Booker SJ. Anaerobic functionalization of unactivated C-H bonds. *Curr. Opin. Chem. Biol.* 2009; 13:58–73. [PubMed: 19297239]
32. Broderick JB, Duffus BR, Duschene KS, Shepard EM. Radical S-Adenosylmethionine enzymes. *Chem. Rev.* 2014; 114:4229–4317. [PubMed: 24476342]
33. The SPASM motif is named after enzymes involved in the maturation of subtilisin A, pyrroloquinoline quinone, anaerobic sulfatase, and mycofactocin maturation. See references 28 and 29.
34. Fang Q, Peng J, Dierks T. Post-translational formylglycine modification of bacterial sulfatases by the radical S-adenosylmethionine protein AtsB. *J. Biol. Chem.* 2004; 279:14570–14578. [PubMed: 14749327]
35. Berteau O, Guillot A, Benjdia A, Rabot S. A new type of bacterial sulfatase reveals a novel maturation pathway in prokaryotes. *J. Biol. Chem.* 2006; 281:22464–22470. [PubMed: 16766528]
36. Benjdia A, et al. Anaerobic sulfatase-maturing enzymes: radical SAM enzymes able to catalyze in vitro sulfatase post-translational modification. *J. Am. Chem. Soc.* 2007; 129:3462–3463. [PubMed: 17335281]
37. Grove TL, Lee KH, St Clair J, Krebs C, Booker SJ. In vitro characterization of AtsB, a radical SAM formylglycine-generating enzyme that contains three [4Fe-4S] clusters. *Biochemistry.* 2008; 47:7523–7538. [PubMed: 18558715]
38. Grove TL, et al. Further characterization of Cys-type and Ser-type anaerobic sulfatase maturing enzymes suggests a commonality in the mechanism of catalysis. *Biochemistry.* 2013; 52:2874–2887. [PubMed: 23477283]
39. Goldman PJ, et al. X-ray structure of an AdoMet radical activase reveals an anaerobic solution for formylglycine posttranslational modification. *Proc. Natl. Acad. Sci. USA.* 2013; 110:8519–8524.
40. Lanz ND, et al. RlmN and AtsB as models for the overproduction and characterization of radical SAM proteins. *Methods Enzymol.* 2012; 516:125–152. [PubMed: 23034227]
41. Johnson DC, Unciuleac MC, Dean DR. Controlled expression and functional analysis of iron-sulfur cluster biosynthetic components within *Azotobacter vinelandii*. *J. Bacteriol.* 2006; 188:7551–7561. [PubMed: 16936042]
42. Wecksler SR, et al. Pyrroloquinoline quinon biogenesis: demonstration that PqqE from *Klebsiella pneumoniae* is a radical S-adenosyl-L-methionine enzyme. *Biochemistry.* 2009; 48:10151–10161. [PubMed: 19746930]
43. Goldman PJ, Grove TL, Booker SJ, Drennan CL. X-ray analysis of butirosin biosynthetic enzyme BtrN redefines structural motifs for AdoMet radical chemistry. *Proc. Natl. Acad. Sci. USA.* 2013; 110:15949–15954. [PubMed: 24048029]
44. Flühe L, et al. Two [4Fe-4S] clusters containing radical SAM enzyme SkfB catalyze thioether bond formation during the maturation of the sporulation killing factor. *J. Am. Chem. Soc.* 2013; 135:959–962. [PubMed: 23282011]
45. Oman TJ, van der Donk WA. Follow the leader: the use of leader peptides to guide natural product biosynthesis. *Nat. Chem. Biol.* 2010; 6:9–18. [PubMed: 20016494]
46. Wu W, Lieder KW, Reed GH, Frey PA. Observation of a second substrate radical intermediate in the reaction of lysine 2,3-aminomutase: a radical centered on the beta-carbon of the alternative substrate, 4-thia-L-lysine. *Biochemistry.* 1995; 34:10532–10537. [PubMed: 7654708]

47. Rusczycky MW, Choi SH, Liu HW. Stoichiometry of the redox neutral deamination and oxidative dehydrogenation reactions catalyzed by the radical SAM enzyme DesII. *J. Am. Chem. Soc.* 2010; 132:2359–2369. [PubMed: 20121093]
48. Grove TL, Ahlum JH, Sharma P, Krebs C, Booker SJ. A consensus mechanism for Radical SAM-dependent dehydrogenation? BtrN contains two [4Fe-4S] clusters. *Biochemistry.* 2010; 49:3783–3785. [PubMed: 20377206]
49. Mitchell J. *Streptococcus mitis*: walking the line between commensalism and pathogenesis. *Mol. Oral Microbiol.* 2011; 26:89–98. [PubMed: 21375700]
50. Le Doare K, Heath PT. An overview of global GBS epidemiology. *Vaccine.* 2013; 31:D7–D12. [PubMed: 23973349]
51. Fittipaldi N, Segura M, Grenier D, Gottschalk M. Virulence factors involved in the pathogenesis of the infection caused by the swine pathogen and zoonotic agent *Streptococcus suis*. *Future Microbiol.* 2012; 7:259–279. [PubMed: 22324994]

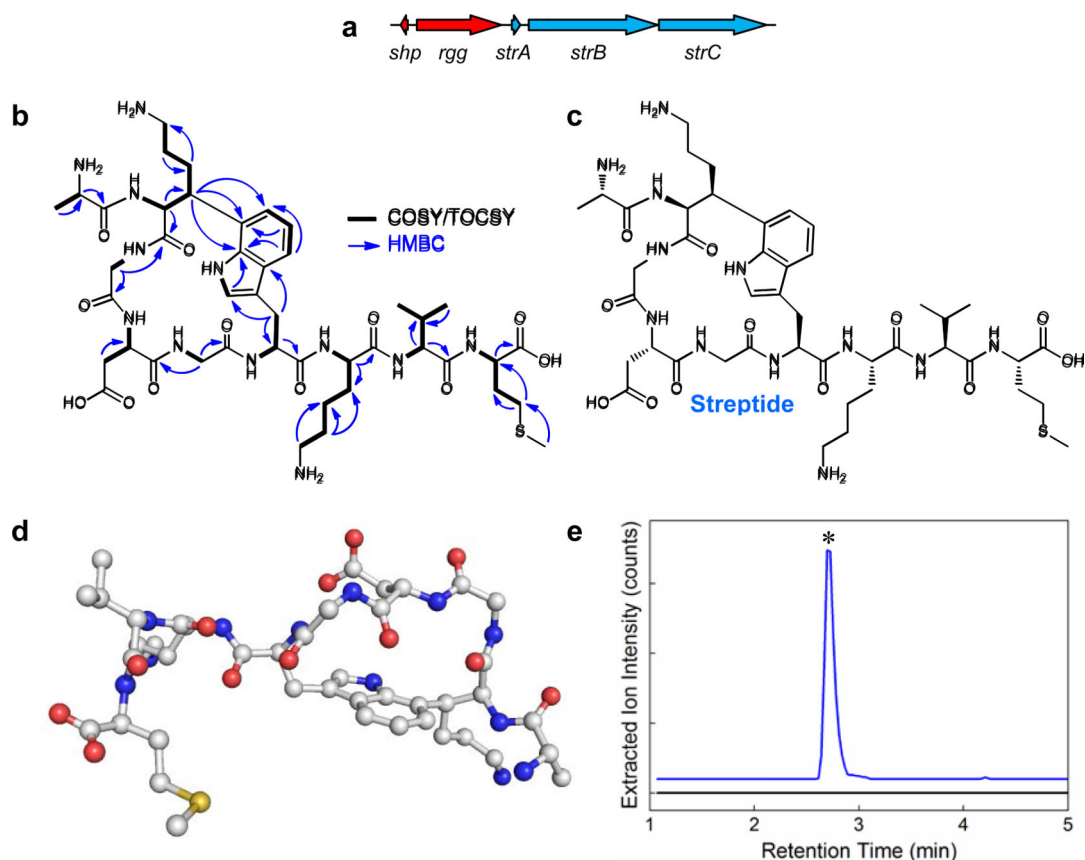


Figure 1. Biosynthetic gene cluster and structure of streptide

a, The *str* cluster consists of a precursor peptide (*strA*), a radical SAM gene (*strB*), and a putative transporter (*strC*). It is activated by the *shp/rgg* quorum sensing system, which encodes a peptide hormone (*shp*) and a transcriptional regulator (*rgg*)¹⁴. **b**, Structural elucidation of streptide by NMR. Key correlations used to solve the structure are indicated. **c**, Structural and stereochemical assignment of streptide. **d**, Computational model of the three-dimensional structure of streptide calculated using CYANA and NMR NOESY constraints. **e**, HR-HPLC-MS analysis of the extracts of wt *S. thermophilus* (red trace) and a *strB::ery* mutant (black trace). Shown is the extracted ion intensity for streptide (m/z 989.4879). The starred peak corresponds to streptide.

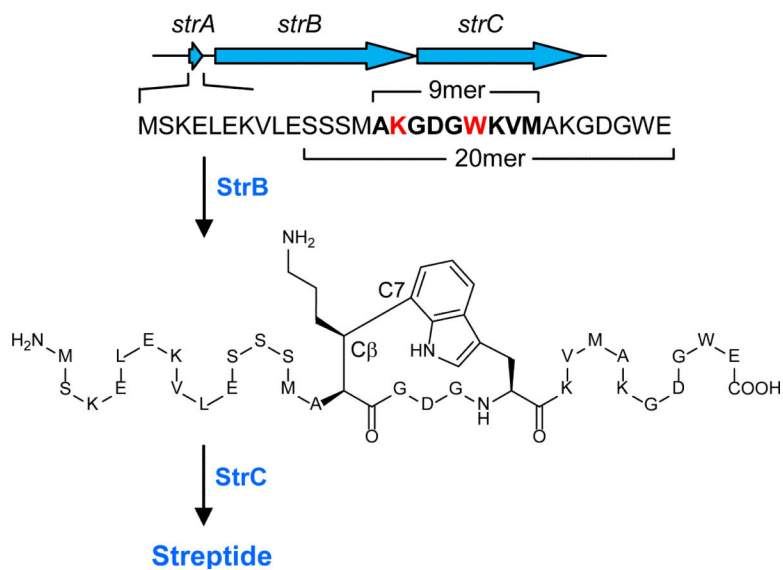


Figure 2. Proposed biosynthesis for streptide

StrA encodes a 30mer substrate. In our model, StrB installs the Lys-to-Trp crosslink, while StrC, possibly in concert with other protease(s), secretes the mature 9mer streptide. A 9mer, 20mer, and the full-length 30mer StrA, synthesized in this study, are shown. The 9mer sequence of streptide is shown in bold; the K and W residues involved in the cyclization are shown in red.

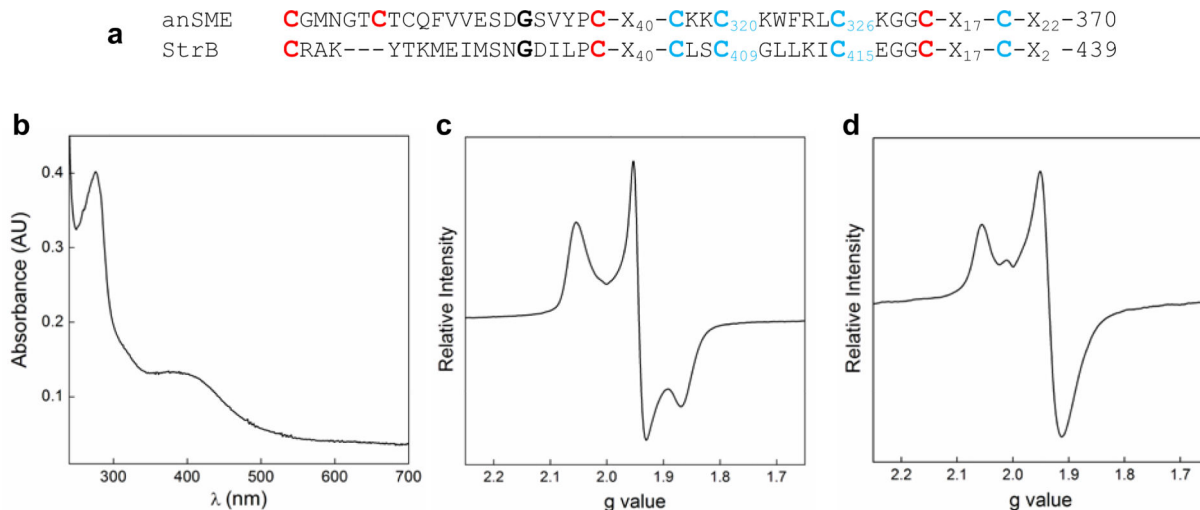


Figure 3. StrB contains two [4Fe-4S] clusters

a, Alignment of the SPASM motif of StrB with that of anSME. Cys residues that bind the AuxI and AuxII clusters (in anSME) are shown in red and blue, respectively. StrB lacks a key Cys ligand to the AuxI cluster. **b**, UV-vis spectrum of reconstituted StrB showing a 320 nm shoulder and a 395 nm feature, characteristic of [4Fe-4S] clusters. **c**, X-band CW EPR spectrum of reconstituted StrB yielding g_x , g_y , and g_z of 1.86, 1.94, and 2.05, respectively. **d**, EPR spectrum of C409A/C415A-StrB with g_{II} and g of 2.06 and 1.93 typical for the SAM-cleaving [4Fe-4S]⁺ cluster.

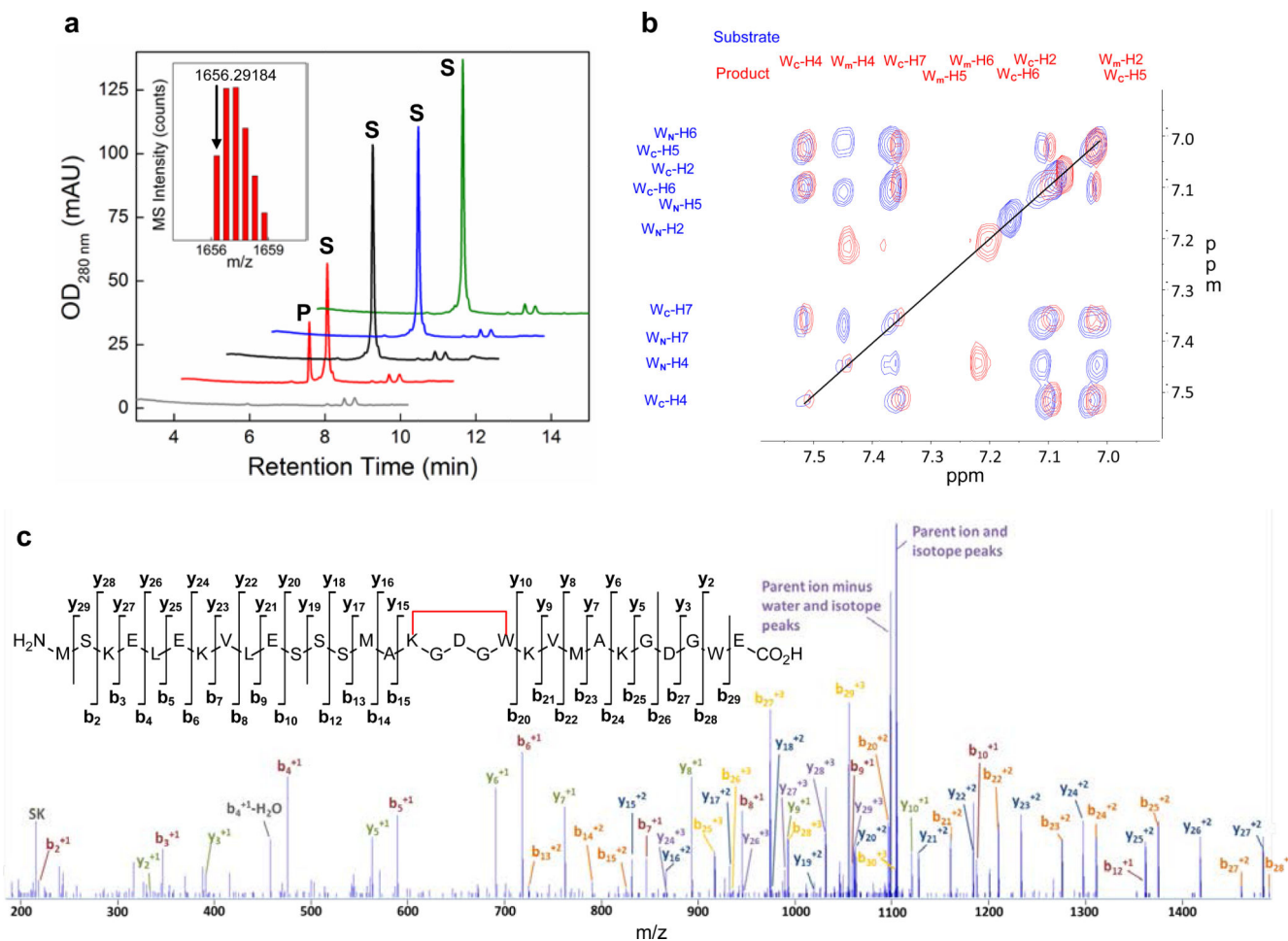


Figure 4. StrB catalyzes Lys-to-Trp crosslink formation in StrA

a. Qtof-HPLC-MS assay for 30mer product formation. Activity assays were carried out in the absence of 30mer substrate (gray trace), reductant (black trace), SAM (blue trace), StrB (green trace), or containing all components (red trace). The 30mer substrate (S) and product (P) peaks are marked. The traces have been offset in both axes for clarity. Inset, HR-ESI-MS spectrum of product 30mer ($[M+2H]^{2+}$ calc 1656.29144). **b.** Overlaid TOCSY NMR spectra of StrA (blue) and the product 30mer (red). The substrate contains two unmodified Trp residues (WC and WN), while the product spectrum reveals a C-terminal Trp (WC) and the modified Trp lacking a ^1H at the indole-C7 (Wm). The peaks have been assigned in the overlaid ^1H traces. See Supplementary Fig. 15 for the upstream region. **c.** HR-MS/MS spectrum of product 30mer. The observed b and y ions are shown in the inset. Fragmentation at all peptide bonds is observed except for those in the KGDGW sequence, consistent with macrocyclization within this motif (see Supplementary Table 5).

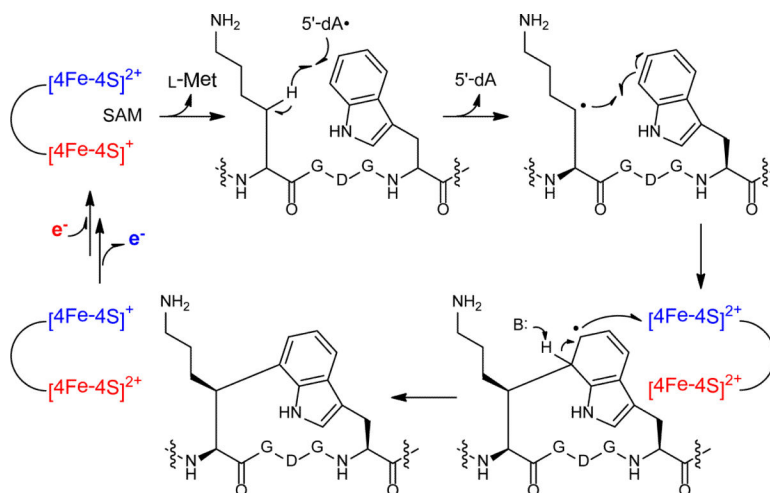


Figure 5. Mechanistic model for Lys-to-Trp crosslink formation catalysed by StrB
 The FeS clusters in red and blue correspond to the SAM-cleaving active site cluster and the auxiliary cluster, respectively. Reductive activation of SAM leads to formation of 5'-dA•, which abstracts a Lys β-hydrogen. The radical thus formed reacts with the indole side chain to create the Lys-to-Trp crosslink and an indolyl radical. Deprotonation and rearomatization with concomitant reduction of the auxiliary Fe-S cluster completes the synthesis of crosslinked StrA.